

**The human cytomegalovirus miR-UL112 synergistically cooperates with a cellular  
microRNA to escape immune elimination**

Daphna Nachmani, Dikla Lankry, Dana G. Wolf and Ofer Mandelboim<sup>1</sup>

**Supplementary web material**

## Supplementary methods

The following oligonucleotides were used to generate artificial short hairpin RNAs that function as orthologs of pre-miRNA hairpins or as a short hairpin RNAs (the sequences of the mature microRNAs are in capitals):

Hsa-miR		5' to 3' sequence
hsa-miR-149	Fw	gatcccc TCTGGCTCCGTGTCTTCACTCCC tcaagaga GGGAGTGAAGACACGGAGCCAGA ttttggaaa
	Rev	agcttttcaaaaa TCTGGCTCCGTGTCTTCACTCCC tctcttgaa GGGAGTGAAGACACGGAGCCAGA ggg
hsa- miR-211	Fw	gatcccc TTCCCTTTGTCATCCTTCGCCT tcaagaga AGGCGAAGGATGACAAAGGGAA ttttggaaa
	Rev	agcttttcaaaaa TTCCCTTTGTCATCCTTCGCCT tctcttgaa AGGCGAAGGATGACAAAGGGAA ggg
hsa-miR-204	Fw	gatcccc TTCCCTTTGTCATCCTATGCCT tcaagaga AGGCATAGGATGACAAAGGGAA ttttggaaa
	Rev	agcttttcaaaaa TTCCCTTTGTCATCCTATGCCT tctcttgaa AGGCATAGGATGACAAAGGGAA ggg
hsa-miR-188	Fw	gatcccc CATCCCTTGCATGGTGGAGGG tcaagaga CCCTCCACCATGCAAGGGATG ttttggaaa
	Rev	agcttttcaaaaa CATCCCTTGCATGGTGGAGGG tctcttgaa CCCTCCACCATGCAAGGGATG ggg
hsa-miR-433	Fw	gatcccc ATCATGATGGGCTCCTCGGTGT tcaagaga ACACCGAGGAGCCCATCATGAT ttttggaaa
	Rev	agcttttcaaaaa ATCATGATGGGCTCCTCGGTGT tctcttgaa ACACCGAGGAGCCCATCATGAT ggg
hsa-miR-376a	Fw	gatcccc ATCATAGAGGAAAATCCACGT tcaagaga ACGTGGATTTTCCTCTATGAT ttttggaaa
	Rev	agcttttcaaaaa ATCATAGAGGAAAATCCACGT tctcttgaa ACGTGGATTTTCCTCTATGAT ggg
hsa- miR-376b	Fw	gatcccc ATCATAGAGGAAAATCCATGTT tcaagaga AACATGGATTTTCCTCTATGAT ttttggaaa
	Rev	agcttttcaaaaa ATCATAGAGGAAAATCCATGTT tctcttgaa AACATGGATTTTCCTCTATGAT ggg
hsa-miR-571	Fw	gatcccc TGAGTTGGCCATCTGAGTGAG tcaagaga CTCACTCAGATGGCCA ACTCA ttttggaaa
	Rev	Agcttttcaaaaa TGAGTTGGCCATCTGAGTGAG tctcttgaa CTCACTCAGATGGCCA ACTCA ggg
kshv-miR- K12-2	Fw	gatcccc CAGATCGACCCGGACTACAGTT tcaagaga AACTGTAGTCCGGGTCGATCTG ttttggaaa
	Rev	Agcttttcaaaaa CAGATCGACCCGGACTACAGTT tctcttgaa AACTGTAGTCCGGGTCGATCTG ggg

Primers used for inserting the hcmv-miR-UL112 binding site into the pGL3 MICB 3' UTR reporter

		5' to 3' sequence
miR-UL112 binding site with BstXI restriction	Fw	ctgg TGCCTGGATCTCACCAGCACTT <i>ccaagtg</i>
	Rev	TTGGAAGTGCTGGTGAGATCCAGGCACCAGCACT

To generate mutated MICB-3'UTR plasmids we used a site directed mutagenesis technique, using the following primers:

		5' to 3' sequence
Mut-433	Fw	GCAAAGGGATCCCGACCAACTCAAC
	Rev	GTTGAGTTGGTCGGGATCCCTTTGC
Mut-376a	Fw	GTTTCCTGACCTCCGAAACAGAG
	Rev	CTCTGTTTCGGAGGTCAGGAAAC

The mut2 mutation in MICB 3'-UTR was generated as described <sup>1</sup>

Primers for miR-17-5p, miR-20a, miR-93, miR-106, miR-372, miR-373 and miR-520d mature microRNA real time were as described<sup>2</sup>

The following primers sequences were used to quantify mature microRNAs levels by qRT-PCR:

	5' to 3' sequence
hU6	ATGACACGCAAATTCGTGAAG
miR-376a	ATCATAGAGGAAAATCCACGT
miR-433	ATCATGATGGGCTCCTCGGTGT

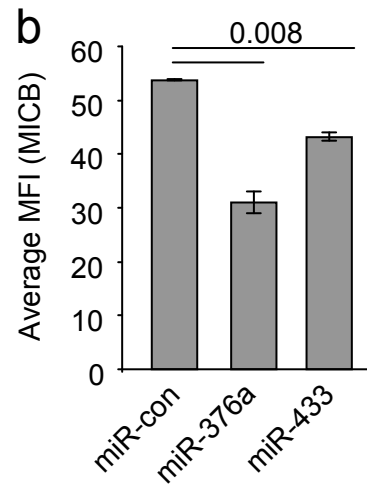
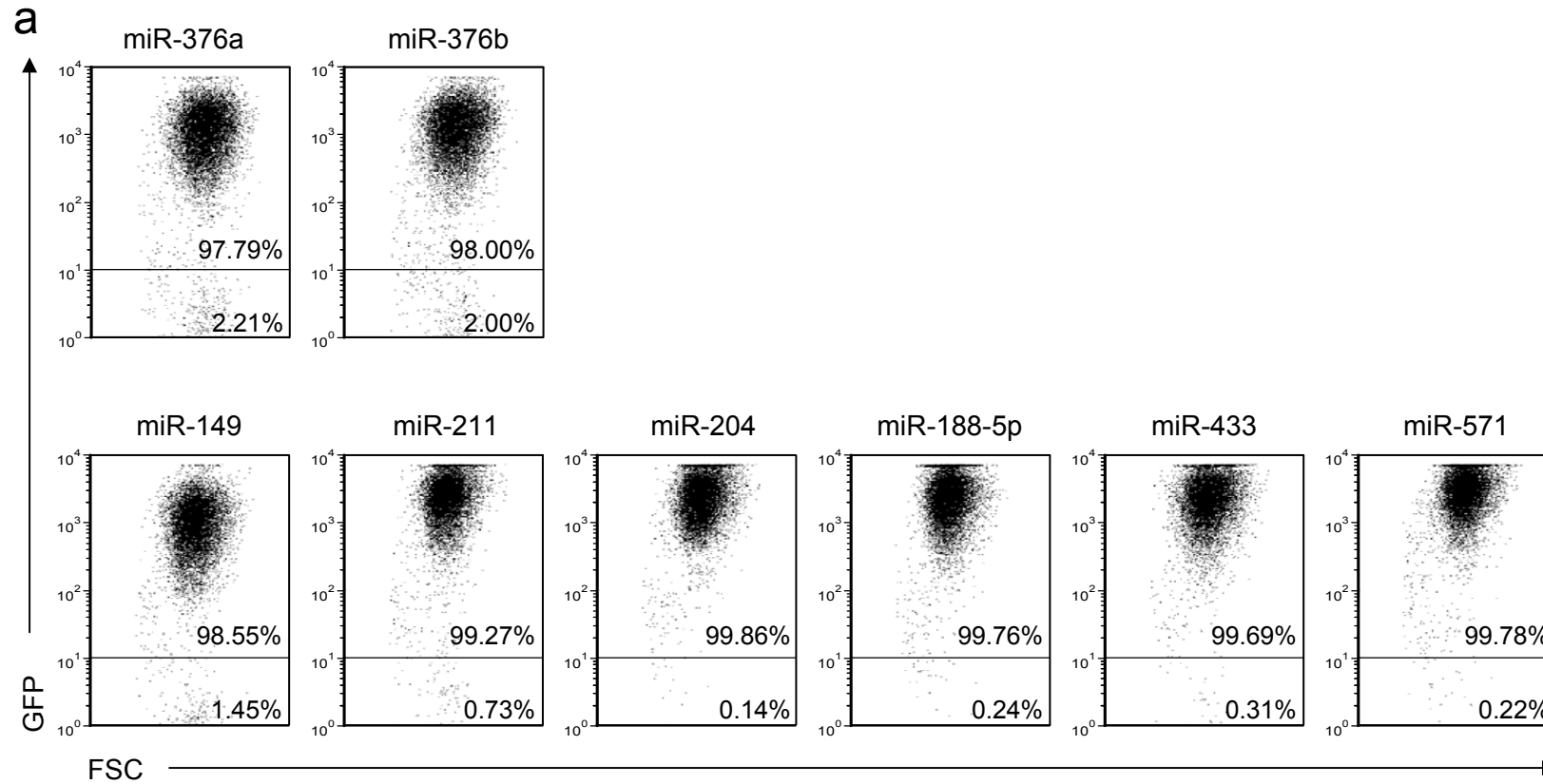
The following primers sequences were used in quantitative real-time PCR analysis of mRNA levels: (MICB as described<sup>2</sup>)

		5' to 3' sequence
hGAPDH	Fw	AACAGCGACACCCACTCCTC
	Rev	CATACCAGGAAATGAGCTTGACAA
hL32	Fw	AGCTCCCAAAAATAGACGCAC
	Rev	TTCATAGCAGTAGGCACAAAGG

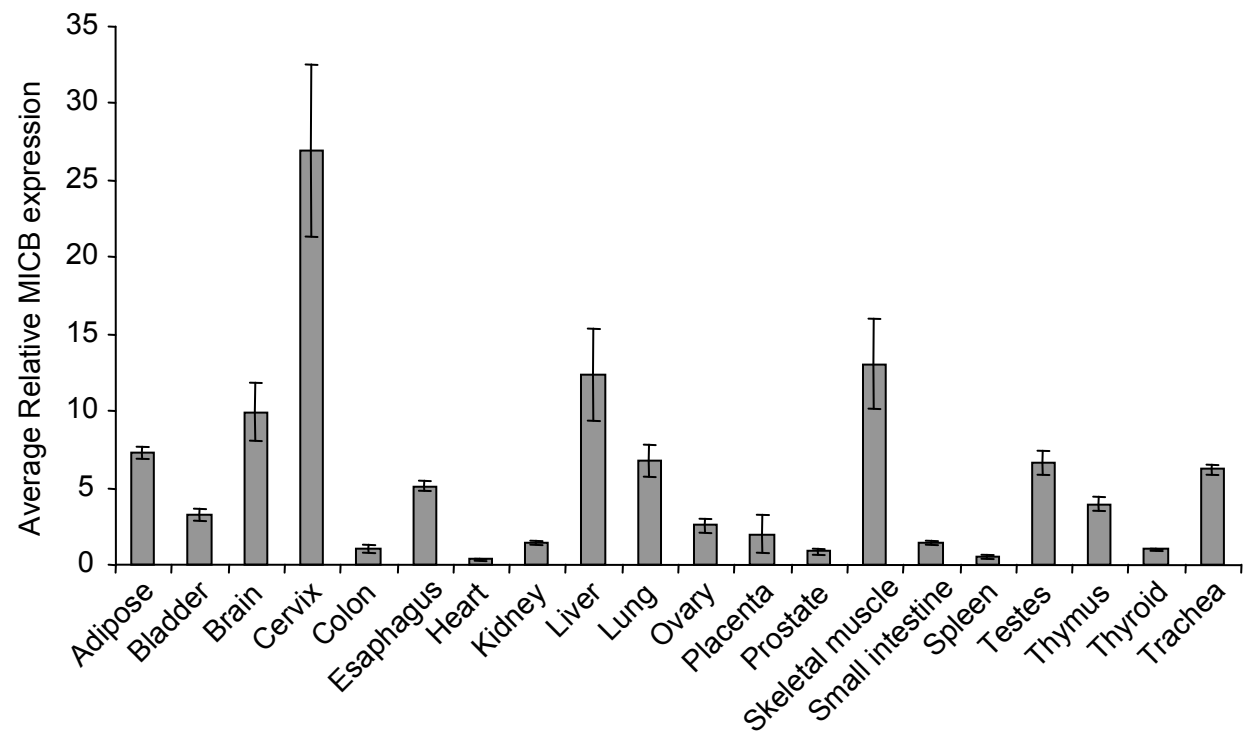
The following oligonucleotides were used to generate the specific anti-miR sponges:

		5' to 3' sequence
anti-miR-376a(1)	Fw	TCGACACGTGGATTGGGTCTATGATAGAGACGTGGATTGGGTCTATGATAGAG ACGTGGATTGGGTCTATGAT A
	Rev	AGCTTATCATAGACCCAATCCACGTCTCTATCATAGACCCAATCCACGTCTCTATCATAGACCCAATCCACGTG
anti-miR-376a(2)	Fw	AGCTTACGTGGATTGGGTCTATGATAGAGACGTGGATTGGGTCTATGATAGAG ACGTGGATTGGGTCTATGAT G
	Rev	AATTCATCATAGACCCAATCCACGTCTCTATCATAGACCCAATCCACGTCTCTATCATAGACCCAATCCACGTGTA
anti-miR-433 (1)	Fw	TCGACACACCGAGGAAAAATCATGATCTCTACACCGAGGAAA AATCATGATCTCTACACCGAGGAAAAATCATGAT A
	Rev	AGCTTATCATGATTTTTTCCTCGGTGTAGAGATCATGATTTTTTCCTCGGTGTAGAGATCATGATTTTTTCCTCGGTGTG
anti-miR-433 (2)	Fw	AGCTTACACCGAGGAAAAATCATGATCTCTACACCGAGGAAA AATCATGAT CTCT ACACCGAGGAAAAATCATGAT G
	Rev	AATTCATCATGATTTTTTCCTCGGTGTAGAGATCATGATTTTTTCCTCGGTGTAGAGATCATGATTTTTTCCTCGGTGTA
anti-miR-UL112 (1)	Fw	TCGACAGCCTGGATCAATCGTCACTTGAGAAGCCTGGATCAA TCGTCACTTGAGA AGCCTGGATCAAT CGTCACTT A
	Rev	AGCTTAAGTGACGATTGATCCAGGCTTCTCAAGTGACGATTG ATCCAGGCTTCTCAAGTGACGATTGATCCAGGCTG
anti-miR-UL112 (2)	Fw	AGCTTAGCCTGGATCAATCGTCACTTGAGAAGCCTGGATCAA TCGTCACTTGAGAAGCCTGGATCAAT CGTCACTT G
	Rev	AATTCAAGTGACGATTGATCCAGGCTTCTCAAGTGACGATTG ATCCAGGCTTCTCAAGTGACGATTGATCCAGGCTA
anti-miR-BART16 (1)	Fw	TCGACAGAGCACACACCGTCCTATCTAATTGGAGAGCACACA CCGTCCTATCTAA TTGG AGAGCACACACCGTCCTATCTAAA
	Rev	GAGAGCACACACCGTCCTATCTAATTGGAGAGCACACACCGT CCTATCTAATTGGAGAGCACACACCGTCCTATCTAATTCGA
anti-miR-BART16 (2)	Fw	AGCTTAGAGCACACACCGTCCTATCTAATTGGAGAGCACACA CCGTCCTATCTAATTGGAGAGCACACACCGTCCTATCTAA G
	Rev	TTAAGTTAGATAGGACGGTGTGTGCTCTCCAATTAGATAGGA CGGTGTGTGCTCTCCAATTAGATAGGACGGTGTGTGCTCTT

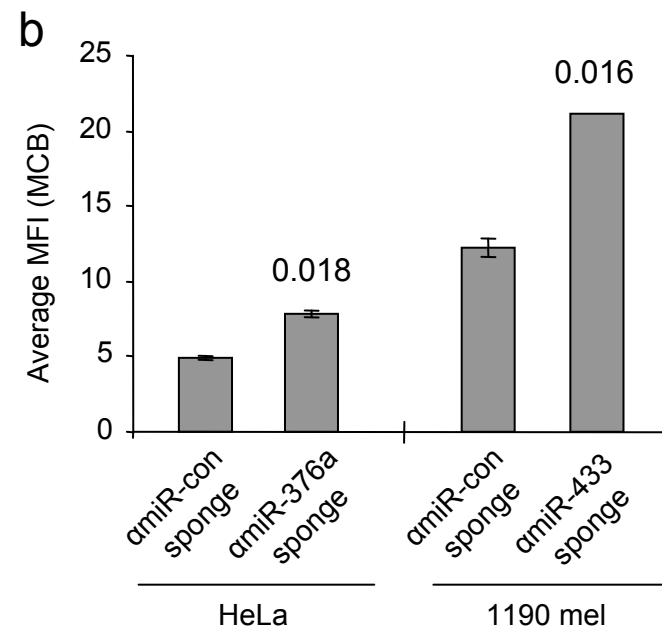
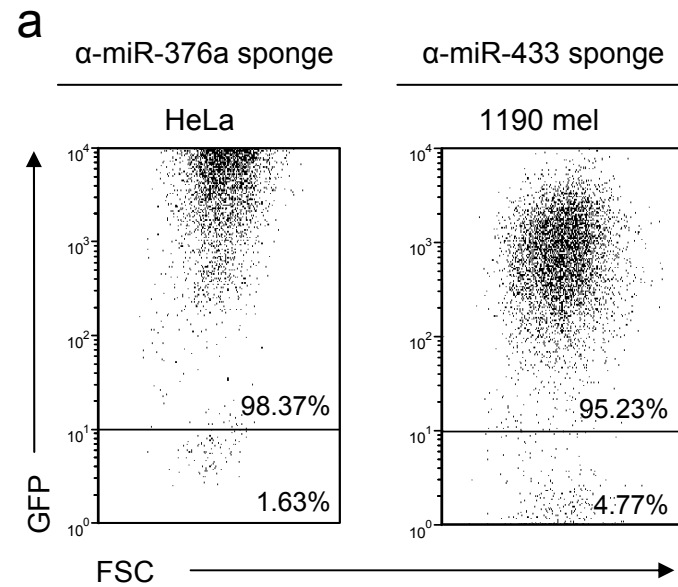
1. Stern-Ginossar, N. *et al.* Host immune system gene targeting by a viral miRNA. *Science* **317**, 376-381 (2007).
2. Stern-Ginossar, N. *et al.* Human microRNAs regulate stress-induced immune responses mediated by the receptor NKG2D. *Nat Immunol* **9**, 1065-1073 (2008).



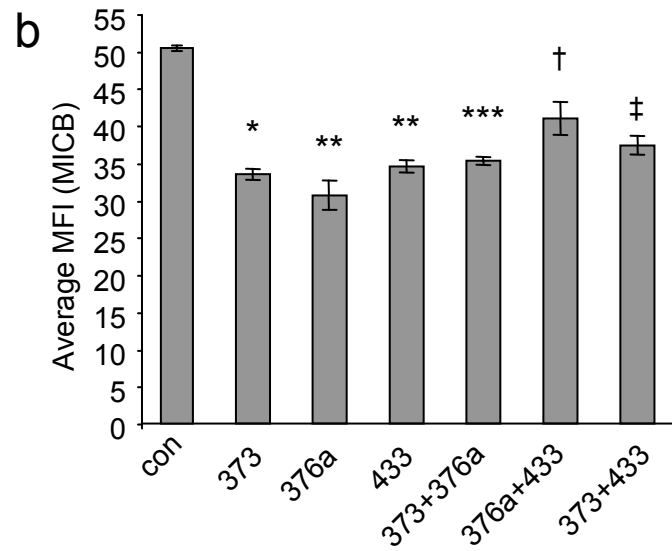
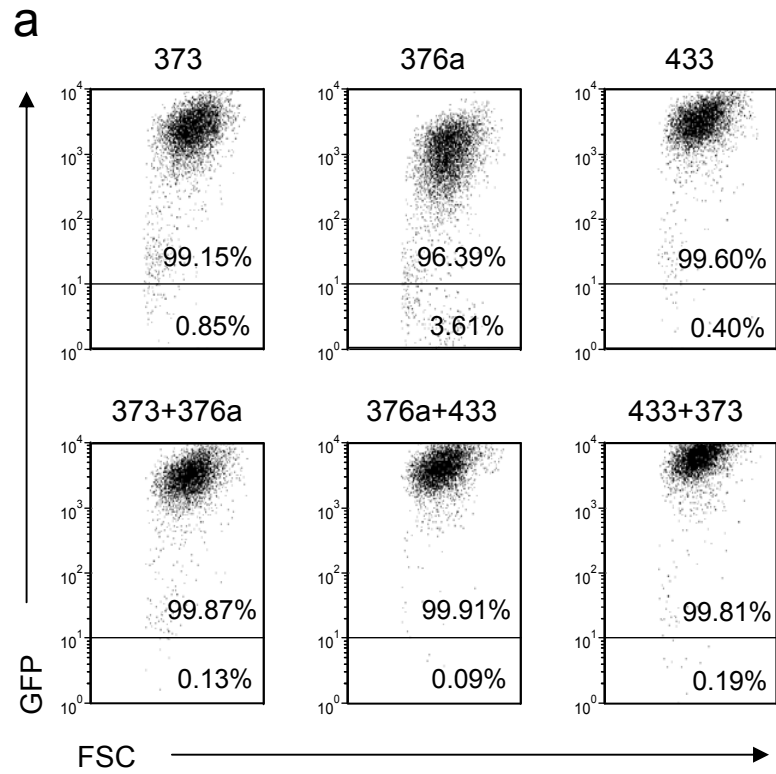
Supp figure 1



Supp Figure 2

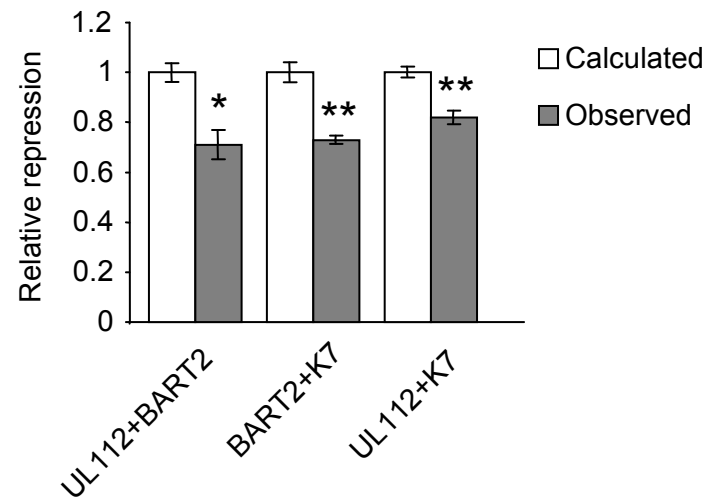


Supp figure 3

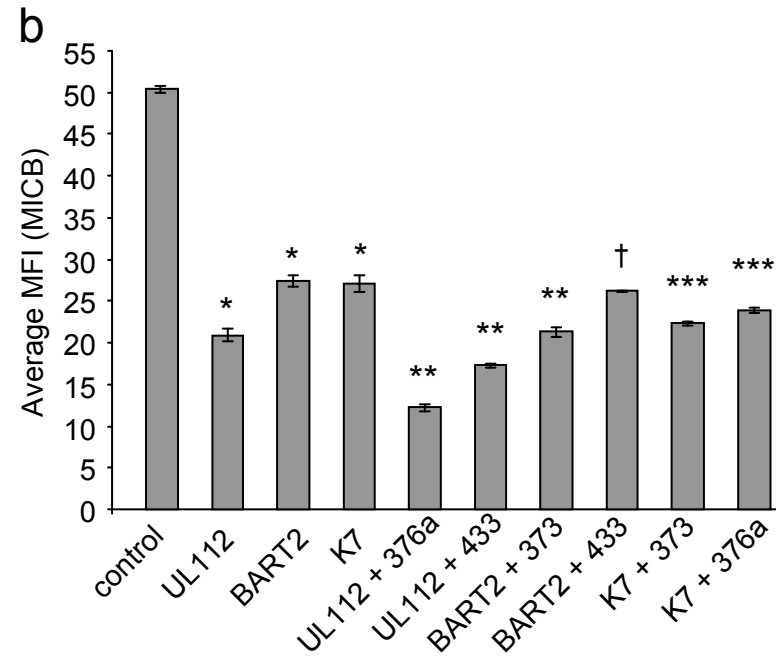
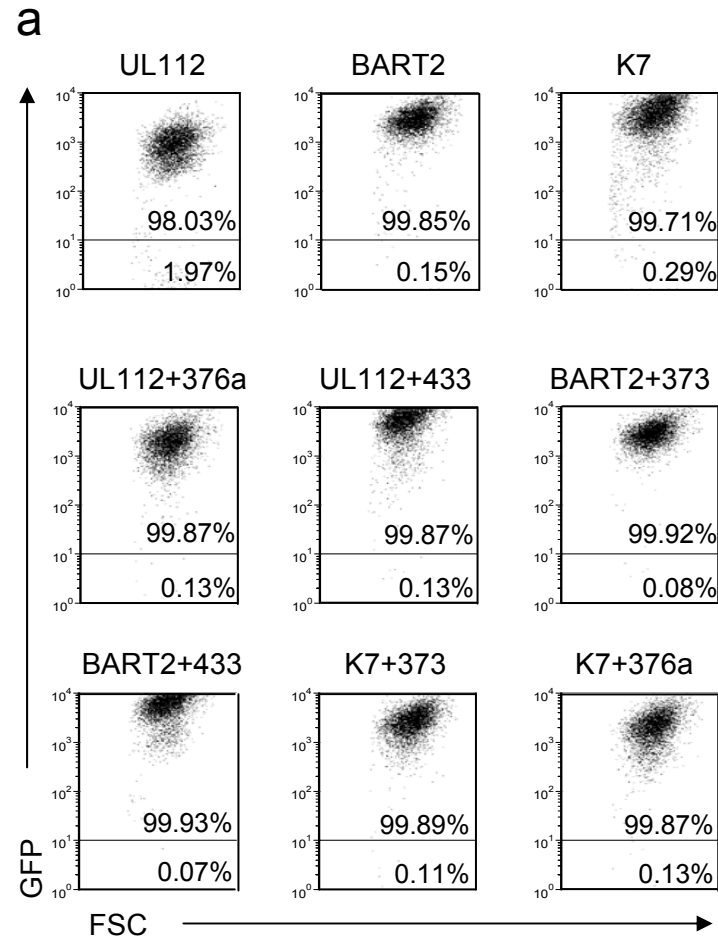


Supp figure 4

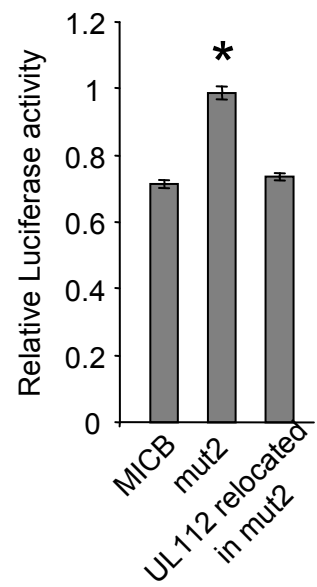




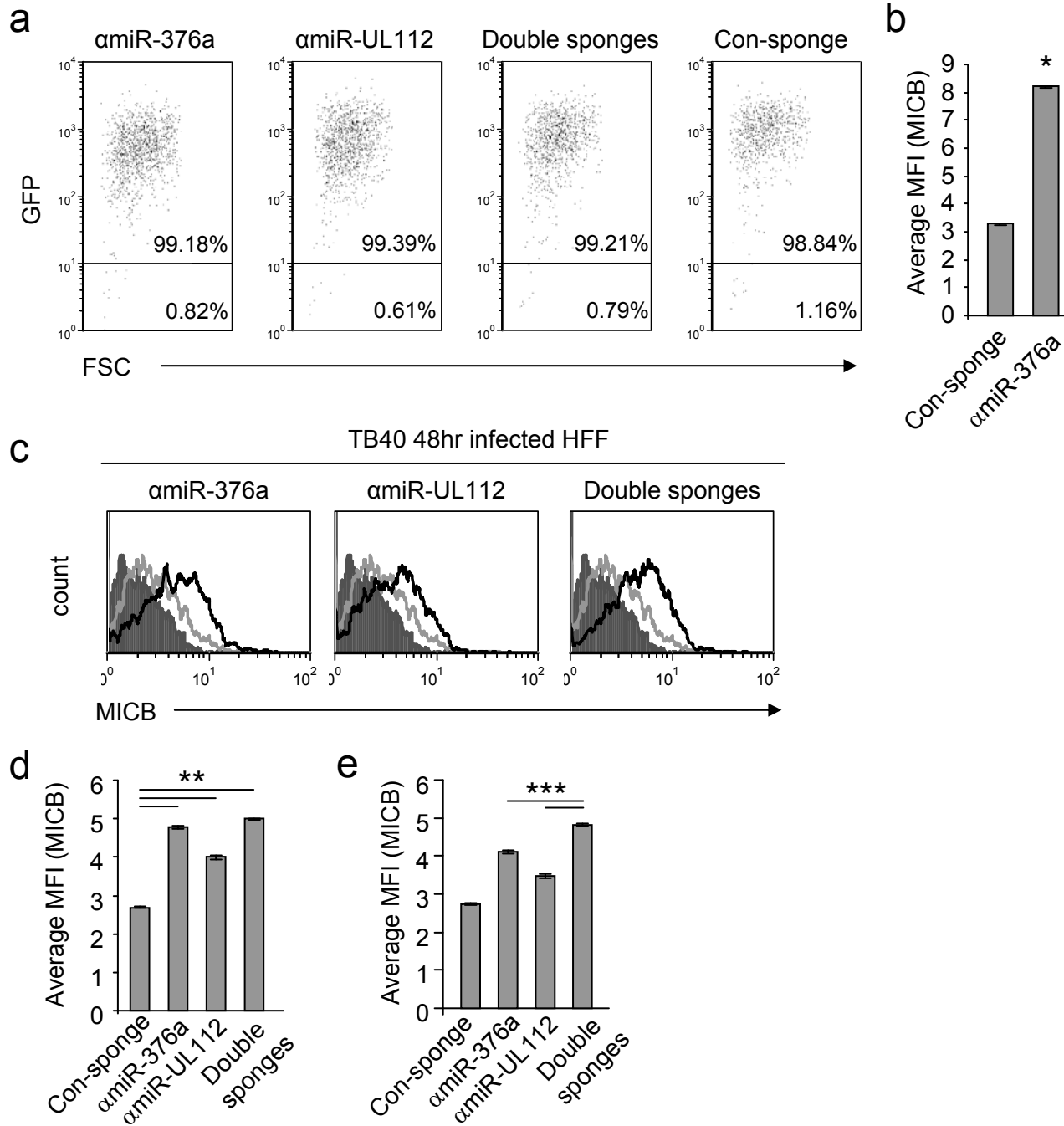
Supp Figure 5



Supp figure 6



Supp Figure 7



Supp Figure 8

detection of miRNA O.E.	miR-UL112	miR-BART2-5p	miR-K7	miR-373	p-value	miR-376a	p-value	miR-433	p-value
miRNA control	N.A	N.A	N.A	35.48±1.13		36.6±0.00		28.19±0.15	
UL112	27.28±0.03								
BART2-5p		27.68±0.09							
K7			27.02±0.08						
373				24.04±0.28	0.0273				
376a						25.83±0.01	0.0002		
433								23.27±0.2	0.0138
373+376a				23.47±0.04	0.0253	25.31±0.1	0.0025		
373+433				26.02±0.06	0.0320			24.69±0.24	0.0215
376a+433						27.65±0.24	0.0073	24.28±0.24	0.0193
UL112+BART2-5p	29.25±0.11	29.14±0.1							
UL112+K7	30.47±0.51		26.72±0.06						
BART2-5p+K7		27.78±0.05	24.51±0.01						
UL112+376a	29.69±0.14					28.35±0.42	0.0138		
UL112+433	30.00±0.04							25.67±0.75	0.0460
BART2-5p+373		28.65±0.06		26.78±0.23	0.0355				
BART2-5p+433		29.53±0.74						24.12±0.4	0.0282
K7+373			25.38±0.04	25.26±0.15	0.0299				
K7+376a			24.96±0.01			26.83±0.17	0.0047		

Supp table 1

hcmv-miR-UL112	-					
ebv-miR-BART2-5p	36	-				
kshv-miR-K12-7	129	93	-			
hsa-miR-373	-	36	129	-		
hsa-miR-376a	24	-	105	24	-	
hsa-miR-433	132	96	-	132	108	-
	hcmv-miR-UL112	ebv-miR-BART2-5p	kshv-miR-K12-7	hsa-miR-373	hsa-miR-376a	hsa-miR-433

Supp table 2

**Supplementary figure 1** GFP expression and MICB downregulation

(a) Transduction efficiency of the various microRNAs measured by the GFP expression levels in the transduced cells presented in figure 1b. The percentages of the positive and negative population are indicated. (b) Statistical analysis of the Average Median Fluorescent Intensity (MFI) of MICB downregulation mediated by miR-376a or miR-433, presented in figure 1b. The statistically significant differences that are indicated were calculated by two-tailed student t-test, shown are the average mean values  $\pm$  SEM (calculated by six independent experiments).

**Supplementary figure 2** The expression pattern of the mRNA of MICB in healthy human tissues.

RNA from healthy human tissues was analyzed for the expression of the MICB transcripts by quantitative real-time PCR. Average relative mRNA abundance is shown relative to the hGAPDH mRNA levels in Thyroid tissue. Shown are average mean values  $\pm$  SEM (calculated by three independent experiments).

**Supplementary figure 3** Sponges expression and MICB upregulation

(a) The transduction efficiency of the anti-miR-376a and anti-miR-433 sponges measured by GFP expression levels in the transduced cells presented in figure 4a. The percentages of the positive and negative population are indicated. (b) Statistical analysis of the effect of the various sponges on the MFI of MICB expression presented in figure 4a. Statistically significant differences that were calculated by two-tailed student t-test are indicated. Shown are average mean  $\pm$  SEM (calculated by three independent experiments).

**Supplementary figure 4** GFP expression of the cellular microRNAs combinations and statistical analysis of MICB downregulation in the various combinations

(a) The transduction efficiency of the various cellular microRNAs combinations presented in figure 5b as measured by GFP expression level in the transduced cells. The percentages of the positive and negative population are indicated. (b) Statistical analysis of the MFI of the MICB downregulation by the single microRNAs, or by the combinations of the co-expression of cellular microRNAs presented in figure 5b. Statistically significant differences are indicated and were calculated by two-tailed student t-test. Shown are average mean  $\pm$  SEM (calculated by four independent experiments). The effect of a single microRNA was calculated relative to the control microRNA \* $P < 0.0005$ , \*\* $P = 0.008$ . In all cases of microRNA combinations a statistically significant MICB repression was observed as compared to the control microRNA. The effect of the microRNA combinations was compared to the single microRNA which gave the most efficient MICB downregulation \*\*\* $P < 0.025$  [relative to the downregulation observed by miR-376a, indicating the antagonistic effect of the combinations], † $P < 0.015$  [relative to the downregulation observed by miR-376a, indicating the antagonistic effect of the combinations], ‡ $P = 0.011$  [relative to the downregulation observed by miR-373, indicating the antagonistic effect of the microRNA combination].

**Supplementary figure 5.** Co-expression of viral microRNAs results in reduced luciferase activity

The figure demonstrates relative luciferase repression after transfection of the MICB 3' UTR reporter plasmid into RKO cells transduced with the indicated pair of microRNAs or with a control-microRNA. The calculated repression is the linear summation of the relative luciferase repression by the single microRNA expressed in RKO cells. The observed



repression is the relative luciferase repression when both microRNAs were expressed in RKO cells. Shown are mean values  $\pm$  SEM (derived from triplicates) of a representative experiments out of three independent experiments performed. Statistically significant differences are indicated (\* $P=0.012$  \*\* $P<0.0015$ , by two-tailed student t-test).

### **Supplementary figure 6** Cellular and viral microRNA cooperation

(a) The transduction efficiency of a single, or of pairs of microRNA expression, presented in figure 6a as measured by GFP expression. The percentages of the positive and negative population are indicated. (b) The statistical analysis of the MFI of MICB downregulation presented in figure 6a, mediated by a single viral microRNA, or by the various viral-cellular pairs. Statistically significant differences are indicated and were calculated by two-tailed student t-test. The effect observed with each of the viral microRNA presented in figure 6a was compared to the control-microRNA. \* $P<0.003$ , indicating that the MICB downregulation is significant. The downregulation of MICB mediated by the various pairs of viral and cellular microRNAs presented in figure 6a was compared to the downregulation mediated by the single corresponding viral microRNA and not to the cellular microRNAs as the downregulation of the viral microRNAs was always more pronounced as compared to the cellular ones (\*\* $P<0.015$ , \*\*\* $P=0.02$ , † $P=0.035$ ). Shown are average mean values  $\pm$  SEM (calculated by three independent experiments).

### **Supplementary figure 7.** The binding site of miR-UL112 is functional after relocation.

The figure demonstrates relative luciferase activity by miR-UL112 after transfection with the indicated reporter plasmids. Mut2 is a reporter plasmid containing the 3' UTR of MICB in which the miR-UL112 seed is mutated. Shown are mean values  $\pm$  SEM (derived from triplicates) of a representative experiments out of three independent experiments

performed. Statistically significant differences are indicated (\*- $P=0.02$ , by two-tailed student t-test).

### **Supplementary figure 8 Sponges and HCMV infection**

(a) The transduction efficiency of all sponge constructs presented in figure 7, measured by GFP expression. The percentages of the positive and negative population are indicated.

(b) The statistical analysis of the MFI of MICB upregulation presented in figure 7a, mediated by the anti-miR-376a sponge. Statistically significant differences are indicated and were calculated by two-tailed student t-test \* $P=0.0037$ . Shown are average mean  $\pm$  SEM (calculated by three independent experiments).

(c) Transduced HFF cells (with the sponge/s indicated above the histogram) were infected with the TB40 strain of HCMV (MOI of 1). 48 hrs post infection the cells were analyzed for their MICB expression. The black empty histogram represents the MICB expression by the infected HFF cells with the indicated sponge/s, the gray empty histogram represents infected HFF cells transduced with a control-sponge. The filled gray histogram is of secondary mAb staining only. A representative of three independent experiments is presented. (d, e) The statistical analysis of the MFI of MICB upregulation by infected HFF cells transduced with the indicated sponges presented in the c part of this supplementary figure and in figure 7b; 48 hrs (d) and 72 hrs (e) post infection. Statistically significant differences are indicated and were calculated by two-tailed student t-test \*\*- $P<6.2*10^{-5}$ , \*\*\*- $P<1.01*10^{-5}$ . Shown are average mean  $\pm$  SEM (calculated by three independent experiments).

**Supplementary table 1.** Validation of the expression of all viral and cellular microRNAs utilized in this manuscript.

Shown are representative mean Ct values  $\pm$  SEM (from three independent experiments). The level of microRNA expression by each cell line was compared to the level of this specific microRNA in the cells transduced with a control-microRNA. Statistical differences were calculated by two-tailed student t-test. Viral microRNAs were not amplified (N.A – not amplified), as they are not endogenously expressed by human cells, thus no statistical analysis is provided for the viral microRNAs. Where combinations of cellular microRNAs are presented, statistical analysis is provided for the expression of each of the microRNA as compared to the expression of the specific microRNA in cells transduced with a control-microRNA. Where combinations of two viral microRNAs are presented no statistical analysis is provided since the viral microRNAs are not expressed in the cell lines. Where combinations of viral and cellular microRNAs are presented the statistical analysis is only provided for the cellular microRNA since no viral microRNAs are present in the cell lines transduced with a microRNA control. O.E. – over expression.

**Supplementary table 2.** Site proximity.

The calculated distances between the various viral and/or cellular microRNAs binding sites in the 3' UTR of MICB. The numbers shown represent the number of nucleotides between the 5' ends of the binding sites.